

# Direct identification of propargyl radical in combustion flames by vacuum ultraviolet photoionization mass spectrometry

T. Zhang, X. N. Tang, K.-C. Lau, and C. Y. Ng<sup>a)</sup>

*Department of Chemistry, University of California at Davis, Davis, California 95616*

C. Nicolas, D. S. Peterka, and M. Ahmed<sup>b)</sup>

*Chemical Science Division, Lawrence Berkeley National Laboratory, Berkeley, California 94720*

Melita L. Morton and Branko Ruscic<sup>c)</sup>

*Chemistry Division, Argonne National Laboratory, Argonne, Illinois 60439-4831*

R. Yang, L. X. Wei, C. Q. Huang, B. Yang, J. Wang, L. S. Sheng, Y. W. Zhang, and F. Qi<sup>d)</sup>

*National Synchrotron Radiation Laboratory, University of Science and Technology of China, Hefei, Anhui 230029, People's Republic of China*

(Received 8 November 2005; accepted 4 January 2006; published online 15 February 2006)

We have developed an effusive laser photodissociation radical source, aiming for the production of vibrationally relaxed radicals. Employing this radical source, we have measured the vacuum ultraviolet (VUV) photoionization efficiency (PIE) spectrum of the propargyl radical ( $C_3H_3$ ) formed by the 193 nm excimer laser photodissociation of propargyl chloride in the energy range of 8.5–9.9 eV using high-resolution (energy bandwidth=1 meV) multibunch synchrotron radiation. The VUV-PIE spectrum of  $C_3H_3$  thus obtained is found to exhibit pronounced autoionization features, which are tentatively assigned as members of two vibrational progressions of  $C_3H_3$  in excited autoionizing Rydberg states. The ionization energy (IE=8.674±0.001 eV) of  $C_3H_3$  determined by a small steplike feature resolved at the photoionization onset of the VUV-PIE spectrum is in excellent agreement with the IE value reported in a previous pulsed field ionization-photoelectron study. We have also calculated the Franck-Condon factors (FCFs) for the photoionization transitions  $C_3H_3^+(\tilde{X}; \nu_i, i=1-12) \leftarrow C_3H_3(\tilde{X})$ . The comparison between the pattern of FCFs and the autoionization peaks resolved in the VUV-PIE spectrum of  $C_3H_3$  points to the conclusion that the resonance-enhanced autoionization mechanism is most likely responsible for the observation of pronounced autoionization features. We also present here the VUV-PIE spectra for the mass 39 ions observed in the VUV synchrotron-based photoionization mass spectrometric sampling of several premixed flames. The excellent agreement of the IE value and the pattern of autoionizing features of the VUV-PIE spectra observed in the photodissociation and flames studies has provided an unambiguous identification of the propargyl radical as an important intermediate in the premixed combustion flames. The discrepancy found between the PIE spectra obtained in flames and photodissociation at energies above the IE( $C_3H_3$ ) suggests that the PIE spectra obtained in flames might have contributions from the photoionization of vibrationally excited  $C_3H_3$  and/or the dissociative photoionization processes involving larger hydrocarbon species formed in flames.

© 2006 American Institute of Physics. [DOI: 10.1063/1.2168448]

## I. INTRODUCTION

The modeling of the reaction kinetics in the combustion of hydrocarbon fuels<sup>1</sup> requires structural identification and concentration measurements of key intermediates produced in hydrocarbon flames under controlled conditions. Many key intermediates, such as hydrocarbon radicals, are known to exist in different isomeric forms. The identification of these intermediates in flames has posed a great challenge to combustion chemists.<sup>2</sup> Since the spectroscopy of most hy-

drocarbon radicals is unknown, the application of conventional optical techniques is limited only to a few diatomic and triatomic species.

By virtue of the high vacuum ultraviolet (VUV) energy resolution and the threshold law for photoionization, the ionization energies (IEs) of molecular species with different isomeric structures can readily be distinguished by VUV-photoionization efficiency (PIE) measurements.<sup>3</sup> This method based on IE determinations by VUV-PIE measurements has been employed previously for the identification of isomeric structures of nascent photoproducts in excimer laser photodissociation studies.<sup>3-5</sup> Recently, the VUV photoionization mass spectrometric sampling technique has also been successfully applied for the identification of flame species using broadly tunable synchrotron radiation.<sup>2,6</sup> Nonetheless,

<sup>a)</sup>Electronic mail: cyng@chem.ucdavis.edu

<sup>b)</sup>Electronic mail: mahmed@lbl.gov

<sup>c)</sup>Electronic mail: ruscic@anl.gov

<sup>d)</sup>Electronic mail: fqj@ustc.edu.cn

the IE determination of molecular species in flames using the VUV-PIE method is expected to be less precise due to high rotational and vibrational hot band effects of flame species. As a result, the IE measurement alone may not be adequate for an unambiguous structural assignment. The comparison between the VUV-PIE curves of flame species and those of molecular species with known chemical structures and temperatures is desirable for reliable chemical structure assignments and quantitative measurements of flame species. The VUV-PIE spectrum of a molecule near its IE measured with a sufficiently high VUV energy resolution is often distinct and can serve as a fingerprint for an unambiguous identification of the molecule in flames or reactive environments.<sup>7</sup> In principle, a VUV-PIE spectrum, which provides relative photoionization cross sections of a molecule, can be converted to an absolute photoionization cross-section curve by calibrating the PIE value to the absolute photoionization cross section measured at a fixed VUV energy.<sup>8</sup>

Considering that the VUV-PIE spectra for many hydrocarbon radicals of importance to hydrocarbon combustion are unknown, we have initiated an effort to measure the PIE and photoelectron spectra of combustion radicals using high-resolution VUV synchrotron radiation. In these experiments, the radicals are prepared in known chemical structures by excimer laser photodissociation of appropriate precursor molecules.<sup>8,9</sup> In addition to determining the precise thermochemical data of combustion radicals and their cations, this effort is aimed to establish a VUV-PIE database for the identification of combustion radicals in ongoing flame-sampling experiments<sup>2,6</sup> using the VUV synchrotron-based mass spectrometric method.

As the smallest  $\pi$ -conjugated hydrocarbon radical, the propargyl radical ( $\text{HC}\equiv\text{C}-\dot{\text{C}}\text{H}_2$ ) is a benchmark system for detailed experimental and theoretical characterizations. For the sake of simplicity, we will use  $\text{C}_3\text{H}_3$  and  $\text{C}_3\text{H}_3^+$  below to represent the structures of the propargyl radical and its cation, respectively. The experimental IE value<sup>10</sup> ( $8.6731\pm 0.0013$  eV) of  $\text{C}_3\text{H}_3$  determined by the pulsed field ionization-photoelectron (PFI-PE) study of Gilbert *et al.* is found to be in excellent agreement with the recent high-level *ab initio* IE prediction<sup>11</sup> of 8.679 eV. The propargyl radical is believed to play an important role in the chemistry occurring in hydrocarbon-rich environments, such as in flames, chemical-vapor depositions, interstellar media, outflows of carbon stars, and planetary atmospheres.<sup>12,13</sup> Furthermore,  $\text{C}_3\text{H}_3$  is recognized to be a precursor in the formation of benzene, polycyclic aromatic hydrocarbons, and soot in flames because the combination of two  $\text{C}_3\text{H}_3$  radicals is expected to promote the formation of the first aromatic ring in one bimolecular step.<sup>14</sup> Soot is carcinogenic and also damaging to combustion engines. Hence, the understanding of soot formation is of vital importance in the study of combustion and environmental chemistry.

This article presents a high-resolution VUV-PIE study of  $\text{C}_3\text{H}_3$  prepared by the 193 nm excimer laser photodissociation of propargyl chloride ( $\text{HC}\equiv\text{C}-\text{CH}_2\text{Cl}$ ). The comparison of this spectrum with the VUV PIE curves for the mass 39 ions observed in selected hydrocarbon flames shows unambiguously that  $\text{C}_3\text{H}_3$  is an important intermediate in these

flames. The VUV-PIE spectrum of  $\text{C}_3\text{H}_3$  has been reported recently in a similar synchrotron-based VUV-PIE experiment by Robinson *et al.*<sup>8</sup> However, the latter experiment mainly concerns the measurement of absolute VUV photoionization cross sections of  $\text{C}_3\text{H}_3$ . Since a low VUV resolution [ $\approx 0.25$  eV, full width at half maximum (FWHM)] was used in Ref. 8, the VUV-PIE spectrum of  $\text{C}_3\text{H}_3$  thus obtained revealed no discernible autoionizing structures.

Although hydrocarbon radicals with a specific isomeric structure can be produced by the 193 nm excimer laser photodissociation of precursor halogenated hydrocarbons, these radicals thus formed may contain significant internal vibrational excitations.<sup>8,9</sup> The recent rovibronic state-selected photoionization studies unambiguously show that the cross section of a molecular species depends on its rovibrational excitations.<sup>15-17</sup> These experiments show that useful photoionization cross sections for radicals must be measured with radicals prepared in a known temperature or a well-defined rovibrational distribution. Here, we also report the design and operation of an effusive radical source based on the excimer laser photodissociation method. By adjusting the frequency of radical-wall collisions in the radical source for efficient vibrational relaxation, thermalized radicals with a temperature close to the wall of the radical source can be achieved. The  $\text{C}_3\text{H}_3$  radicals prepared using this excimer dissociation radical source are expected to have a rovibrational temperature close to room temperature.

## II. EXPERIMENTAL CONSIDERATIONS

The experiment described in the present study concerns two types of synchrotron-based VUV mass spectrometric measurements.

### A. VUV-PIE measurement of the propargyl radical

The present VUV-PIE measurement of  $\text{C}_3\text{H}_3$  was carried out using the VUV photoionization octopole-quadrupole mass spectrometer<sup>18,19</sup> of endstation-2 and the high-resolution VUV undulator synchrotron photoionization source<sup>20</sup> of the Chemical Dynamics Beamline<sup>18</sup> at the Advanced Light Source (ALS). Here, the radio-frequency octopole ion guide of the octopole-quadrupole mass spectrometer was used as a part of the ion lenses for transporting photoions from the photoionization region to the quadrupole mass spectrometer (QMS). As described below, an effusive source of  $\text{C}_3\text{H}_3$  radicals based on the 193 nm excimer laser photodissociation of propargyl chloride was installed for the present study.

The ALS ring was operated in the multibunch mode with the frequency of  $\approx 488$  MHz. In this experiment, Ar was used in the harmonic gas filter to suppress the higher undulator harmonics with photon energies greater than 15.76 eV.<sup>21</sup> Using the 6.65 m Eagle monochromator equipped with a 1200 lines/mm grating and monochromator entrance/exit slit sizes of 100/100  $\mu\text{m}$ , the VUV optical bandwidth was estimated to be 1 meV (FWHM). The dispersed VUV radiation emerging from the monochromator was focused into the photoionization region of the octopole-

quadrupole mass spectrometer, where the intersection of the dispersed VUV beam and the effusive radical beam results in the photoionization of the radicals.

The pseudocontinuous radical source<sup>22,23</sup> employed in the present study was designed and used previously by Ruscic *et al.* at the Argonne National Laboratory. The radical source consists of a quartz capillary (length=12.8 cm, inner diameter=0.38 cm) pointing at the photoionization region. Precursor molecules (propargyl chloride) enter the quartz capillary from the side arm and flow continuously from the quartz capillary into the photoionization region in the form of an effusive beam. The 193 nm ArF excimer laser (GAM Laser Inc.) beam was focused by a quartz lens before traversing the photoionization region and counterpropagating against the effusive precursor beam to enter the quartz tube. The excimer laser beam was aligned by passing it through a window at the opposite end of the quartz tube and subsequently exiting a quartz window located on the top of the experimental chamber. The excimer laser was operated at a pulsed energy of  $\approx 5$  mJ/pulse and a repetition rate of 200 Hz. The relatively long quartz tube used here is designed to promote the relaxation of the vibrationally excited radicals formed in photodissociation processes. By choosing an appropriate density of the precursor molecules in the tube, radical loss due to secondary reactions can be minimized while maintaining sufficient radical-wall collisions for vibrational relaxation of hot radicals. Thus, the effusive radicals entering the photoionization region would have a temperature close to that of the quartz tube. Because of the large overlapping volume of the precursor molecules and the excimer laser beam, radicals formed by photodissociation in the quartz tube were found to effuse into the photoionization region with a time constant of several milliseconds. This, together with the high repetition rate of the excimer laser, results in a pseudocontinuous effusive beam of radicals. The radical source has also been operated successfully using a repetition rate of 400 Hz for the 193 nm excimer laser. During the experiment, the pressure in the photoionization chamber was maintained at  $\leq 2 \times 10^{-6}$  Torr.

Using a QMS allows the detection of photoions in a continuous mode. In the present experiment, the time-of-flight (TOF) profiles of mass-selected ions formed by VUV photoionization of radicals at fixed VUV energies were recorded using a multichannel scaler (MCS) with a channel width of 256 ns. The TOF measurement was triggered by firing of the excimer laser, which is defined to be “time zero” of the TOF scale. Since the excimer laser beam passes through the photoionization region, background  $C_3H_3^+$  ions can be produced by the 193 nm multiphoton photodissociation/photoionization of propargyl chloride molecules. Nevertheless, the photoion signal corresponding to the radicals of interest can be distinguished from the ion background produced by excimer laser ionization by ion TOF analyses described below.

Figure 1(a) shows the TOF spectrum of  $C_3H_3^+$  (mass 39) obtained for an accumulation time of 5 s with both the VUV beam and the excimer laser beam on. The VUV photon energy was set at 8.71 eV, which is slightly above the IE of  $C_3H_3$ . The fact that the excimer laser is operated at a repeti-

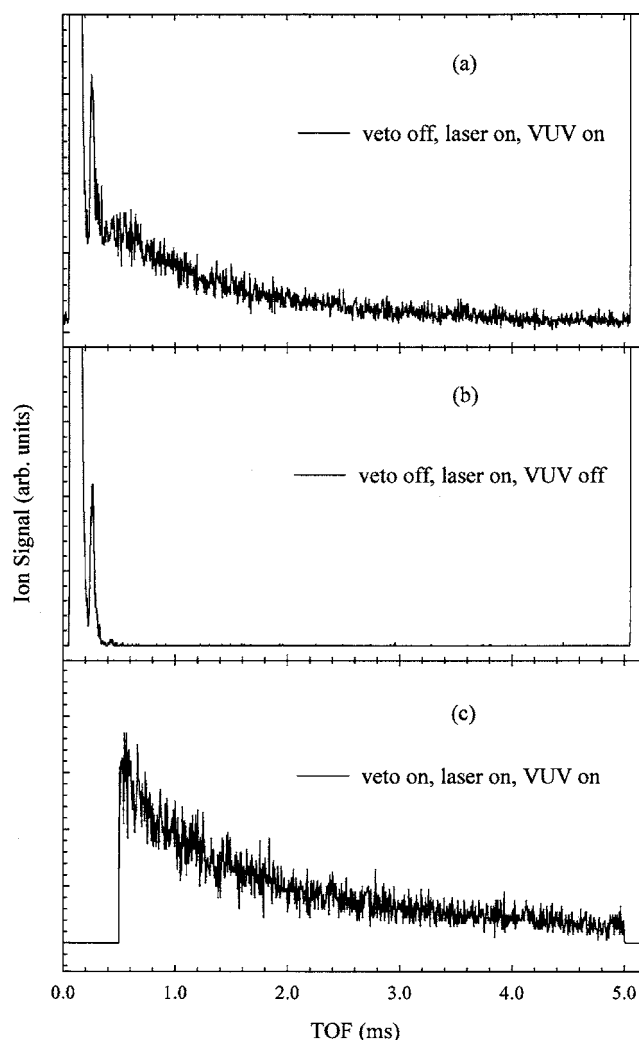


FIG. 1. TOF spectra of the mass 39 cation ( $C_3H_3^+$ ) observed (a) when both the VUV synchrotron light and the 193 nm laser beam were on; (b) when the VUV synchrotron light was off and the 193 nm excimer laser was on; and (c) when both the VUV synchrotron light and the 193 nm laser beam were on, along with the “veto” command that deletes the ion background in the region of 0–500  $\mu$ s. In this experiment, we use a repetition rate of 200 Hz for the 193 nm excimer laser, resulting in the ion detection period of 5 ms. Note that the signal for the mass 39 cations was found to be distributed in the full period of 5 ms. This TOF spectrum of (b) shows that the strong ion peaks appearing in the temporal range of 0–300  $\mu$ s were due to the background ions produced by the excimer-laser multiphoton dissociation/ionization of propargyl chloride. The TOF spectrum of (c) is attributed to photoions formed by the VUV photoionization of  $C_3H_3$ , which is prepared by the 193 nm photodissociation of propargyl chloride.

tion rate of 200 Hz gives a temporal interval of 5 ms between adjacent laser pulses. Thus, the temporal range of 0–5.1 ms covered by the TOF spectrum of Fig. 1(a) consists of more than one detection cycle. Figure 1(b) shows the TOF spectrum for  $C_3H_3^+$  observed with the excimer laser beam on and the VUV beam off. The comparison of the TOF spectra of Figs. 1(a) and 1(b) indicates that the strong ion peak appearing in the early part ( $< 500 \mu$ s) of each ion TOF detection cycle arise from the ion background induced by the 193 nm multiphoton dissociation/ionization processes of propargyl chloride. To avoid the detection of the background ions, a “veto” command was used to stop the ion detector for 500  $\mu$ s after the laser was fired in each ion-detection cycle.

TABLE I. Flow rates for the fuel, O<sub>2</sub>, diluent Ar, and shrouded Ar, and chamber pressures for the four flames examined in the present experiment. The flow rates for O<sub>2</sub>, diluent Ar, and shrouded Ar are in standard liters per min (SLM).

Flame	Fuel flow rate (ml/min)	Diluent Ar flow rate (SLM)	O <sub>2</sub> flow rate (SLM)	Shroud Ar flow rate (SLM)	Pressure of flame chamber (Torr)
Benzene	0.70	1.10	0.80	2.00	35.0
Gasoline	0.45	1.60	0.80	2.00	25.0
Gasoline+5% ethanol	0.45	1.60	0.80	2.00	25.0
Gasoline+5% MTBE	0.45	1.60	0.80	2.00	25.0

A TOF spectrum for C<sub>3</sub>H<sub>3</sub><sup>+</sup> using the veto command with both the VUV beam and the 193 nm excimer beam on is depicted in Fig. 1(c). The ions observed in the latter TOF spectrum can be attributed to C<sub>3</sub>H<sub>3</sub><sup>+</sup> ions formed by VUV photoionization of C<sub>3</sub>H<sub>3</sub> in one detection cycle. That is, the sum of the C<sub>3</sub>H<sub>3</sub><sup>+</sup> ion counts observed in the MCS channels represents the intensity for C<sub>3</sub>H<sub>3</sub><sup>+</sup> ions from VUV photoionization of C<sub>3</sub>H<sub>3</sub>. The measurement of the C<sub>3</sub>H<sub>3</sub><sup>+</sup> ion intensity [ $I(\text{ion})$ ] normalized with the VUV photon intensity [ $I(h\nu)$ ] as a function of VUV photoionization energy [ $h\nu(\text{VUV})$ ] yields the PIE spectrum of C<sub>3</sub>H<sub>3</sub>. We note that the VUV photon detector used here is a photoelectric detector made of polished Cu metal. The VUV detection efficiencies of the Cu photoelectron detector have been normalized by the known photoelectron emission efficiencies of Cu.<sup>21</sup> The VUV-PIE spectra for many molecular species obtained using this calibrated Cu photoelectric detector are found to be consistent with those obtained using a sodium-salicylate-coated photomultiplier. The latter detector is known to have a nearly constant detection efficiency in the VUV range of 30–160 nm.<sup>24</sup>

Using similar experimental procedures, we have measured the VUV-PIE spectra of other radicals, such as methyl radical (CH<sub>3</sub>), chloroformyl radical (CICO), and phenyl radical (C<sub>6</sub>H<sub>5</sub>), demonstrating that the radical source described here is generally useful for producing thermalized radicals for photoionization studies.<sup>23</sup> The simulation of the PIE onset for the CH<sub>3</sub> radical indicates that the CH<sub>3</sub> radicals prepared by the present radical source by the 193 nm excimer photodissociation reactions, CH<sub>3</sub>COCH<sub>3</sub>+ $h\nu(193\text{ nm})\rightarrow\text{CH}_3+\text{CH}_3\text{CO}$  and/or 2CH<sub>3</sub>+CO, have no apparent vibrational excitations and a rotational temperature of  $\approx 150\text{ K}$ .

## B. VUV photoionization mass spectrometric sampling of combustion flames

The experimental arrangement and procedures used for VUV photoionization sampling of the low-pressure premixed flames are similar to those<sup>2,6</sup> reported previously. Briefly, the apparatus consists of a low-pressure flat flame burner situated in the flame chamber, a differentially pumped flame-sampling system, and a reflectron TOF mass spectrometer (RTOF-MS). The ionization chamber was coupled to a 1 m windowless Seya-Namioka monochromator for the dispersion of VUV synchrotron radiation from a bending magnet beamline of the 800 MeV electron storage ring at the National Synchrotron Radiation Laboratory (NSRL) of the Uni-

versity of Science and Technology of China. Using a 1200 lines/mm grating [nominal wavelength resolution = 0.2 nm (FWHM)], the photon intensities were measured to be  $\approx 10^{10}$  photons/s in the VUV range of 7–11 eV.

The premixed laminar flame was stabilized on a 6.0-cm-diameter flat flame burner (McKenna, USA). Movement of the burner towards or away from the quartz sampling cone allowed the TOF mass spectrum to be taken at different positions in the flame. The flame sampling was accomplished using a quartz cone with an orifice of 0.3 mm in diameter mounted on a water-cooled flange. The flame-sample beam thus formed was skimmed by a conical skimmer (diameter = 2 mm) located 15 mm downstream from the sampling cone orifice before intersecting the dispersed VUV synchrotron beam in the photoionization region of the RTOF-MS. The resulting photoions formed by VUV photoionization of flame species were detected by the RTOF-MS, which was operated at a mass resolving power of  $m/\Delta m \approx 1000$ .

The ion TOF mass spectrometric spectrum was measured using a multichannel scaler (FAST Comtec P7888, Germany; total channels=50 000, channel width=1 ns), which was initiated by a delay pulse generator operated at a repetition rate of 18 kHz. The trigger pulse from the delay generator was also used to control the application of a voltage pulse (amplitude=160 V, pulse width=1500 ns) to the repeller plate of the photoionization region for extraction of photoions to be detected by the RTOF-MS. To eliminate the second- and higher-order VUV radiation at wavelengths shorter than 105.0 nm, a lithium fluoride window (thickness=1 mm) was inserted into the VUV beam path. A silicon photodiode (SXUV-100, International Radiation Detectors, Inc., USA) was used to record the VUV photon intensities. The VUV-PIEs for the mass 39 ions reported here were normalized by the corresponding VUV photon intensities after taking into account the known VUV detection efficiencies of the silicon photodiode.

In this work, we have examined the formation of C<sub>3</sub>H<sub>3</sub> in four low-pressure, premixed laminar flames. Flow rates in standard liters per minute (SLM) for O<sub>2</sub>, diluent Ar, and shrouded Ar are controlled independently by separate MKS mass flow controllers. The injection rate (ml/min) of liquid fuels into the vaporizer was controlled by a syringe pump (ISCO 1000D, USA). The standard unblended gasoline was provided by Fangyuan Inc., Liaoning, China. The flame conditions (flow rates for the fuel, O<sub>2</sub>, diluent Ar, and shrouded

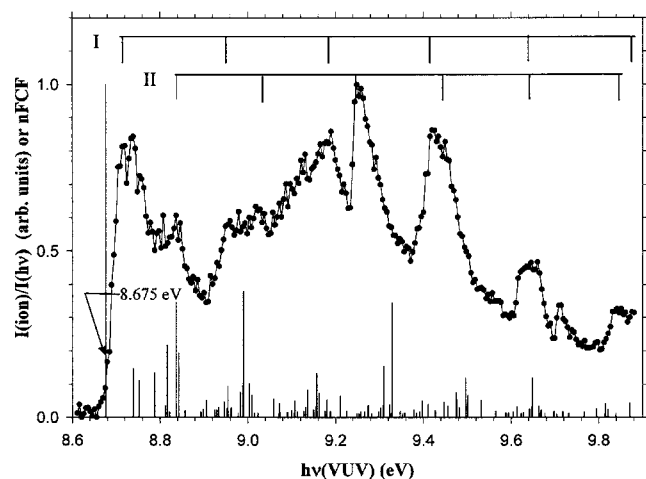


FIG. 2. VUV-PIE spectrum of  $C_3H_3$  in the VUV region of 8.60–9.90 eV obtained using an energy step size of 5 meV. The autoionizing Rydberg peaks tentatively assigned to progressions I and II are marked. The shoulder structure at  $8.675 \pm 0.005$  eV is assigned as the steplike structure that marks the IE of  $C_3H_3$ .

Ar) for the four premixed flames, i.e., the benzene/ $O_2$  flame (flame I), the gasoline/ $O_2$  flame (flame II), the gasoline/5% MTBE/ $O_2$  flame (flame III), and the gasoline/5% ethanol/ $O_2$  flame (flame IV), examined here are given in Table I. Here, MTBE represents methyl tert-butyl ether.

### III. RESULTS AND DISCUSSION

Figure 2 depicts the VUV-PIE spectrum of  $C_3H_3$  in the VUV energy range of 8.60–9.90 eV obtained using an energy step interval of 5 meV. This spectrum exhibits pronounced autoionization structures, which are not observed in the VUV-PIE spectrum<sup>8</sup> of  $C_3H_3$  reported previously by Robinson *et al.* The high-resolution photoelectron spectrum of  $C_3H_3$  has also been recorded by Gilbert *et al.*<sup>10</sup> using the nonresonant two-photon PFI-PE method, yielding a precise value for the IE of  $C_3H_3$ . A careful examination of the ionization onset of the VUV-PIE spectrum reveals a shoulder at  $8.675 \pm 0.005$  eV as shown by an arrow in Fig. 2, which is interpreted as the steplike feature marking the IE of  $C_3H_3$ . In order to examine this shoulder feature in more detail, we show in Fig. 3 the VUV-PIE spectrum of the propargyl radical in the energy range of 8.56–8.80 eV measured using an energy step size of 1 meV. As expected, the steplike feature (marked by a downward arrow in Fig. 3) is more evident; and the position of this steplike feature is located more precisely at  $8.674 \pm 0.001$  eV. Taking the latter value as the IE of  $C_3H_3$ , we find that it is in excellent agreement with the value  $8.673 \pm 0.001$  eV determined in the previous<sup>10</sup> PFI-PE study.

The autoionizing features resolved in Fig. 2 are quite broad. We have been able to group these autoionizing peaks into vibrational progressions I and II. The autoionizing peak positions and vibrational spacings ( $\Delta E$ 's) of these vibrational progressions are listed in Table II. The average  $\Delta E$  spacings for progressions I and II are found to be  $\langle \Delta E \rangle = 0.231$  eV ( $1863$   $cm^{-1}$ ) and  $0.201$  eV ( $1621$   $cm^{-1}$ ), respectively. These autoionizing vibrational features most likely converge to excited vibronic states of  $C_3H_3^+$ . The average  $\langle \Delta E \rangle$  values for

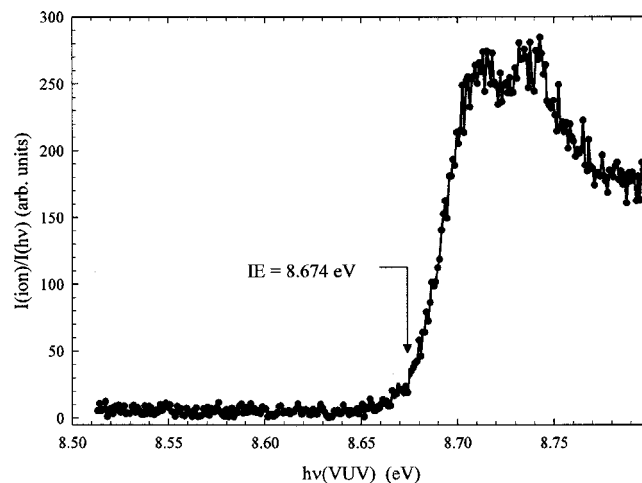


FIG. 3. VUV-PIE spectrum of  $C_3H_3$  near its ionization threshold in the VUV region of 8.51–8.91 eV obtained using an energy step size of 1 meV. The steplike feature at  $8.674 \pm 0.001$  eV marks the IE of  $C_3H_3$ .

progressions I and II are found to fall in between the vibrational frequencies  $\nu_9^+$  (C–C–C stretch) =  $2122$   $cm^{-1}$  and  $\nu_8^+$  ( $CH_2$  scissors) =  $1465$   $cm^{-1}$  for  $C_3H_3^+$  in its ground electronic state, which were determined in the previous PFI-PE study.<sup>10</sup> Considering this observation, we have tentatively associated these vibrational progressions I and II with the excitation of the C–C–C stretching and the  $CH_2$  scissors vibrational modes of  $C_3H_3$  in excited Rydberg states, respectively.

To shed light on the mechanism for the formation of autoionization features resolved in Fig. 2, we have calculated the Franck-Condon factors (FCFs) for the photoionization transitions  $C_3H_3^+(\tilde{X}; \nu_i; i=1-12) \leftarrow C_3H_3(\tilde{X})$ , where  $\nu_i$ ,  $i=1-12$  are the normal vibrational modes for  $C_3H_3^+$ .<sup>25</sup> The calculation uses theoretical anharmonic frequencies [ $\nu_1(b_1) = 278$   $cm^{-1}$ ,  $\nu_2(b_2) = 331$   $cm^{-1}$ ,  $\nu_3(b_2) = 618$   $cm^{-1}$ ,  $\nu_4(b_1) = 899$   $cm^{-1}$ ,  $\nu_5(b_2) = 1014$   $cm^{-1}$ ,  $\nu_6(b_1) = 1113$   $cm^{-1}$ ,  $\nu_7(a_1) = 1139$   $cm^{-1}$ ,  $\nu_8(a_1) = 1440$   $cm^{-1}$ ,  $\nu_9(a_1) = 2089$   $cm^{-1}$ ,  $\nu_{10}(a_1) = 2976$   $cm^{-1}$ ,  $\nu_{11}(b_2) = 3059$   $cm^{-1}$ , and  $\nu_{12}(a_1) = 3226$   $cm^{-1}$ ] for  $C_3H_3^+$  obtained at the Becke three-parameter Lee-Yang-Parr (B3LYP)/6-311G(2df,p) level. The available experi-

TABLE II. Members of autoionizing Rydberg vibrational progressions I and II and their vibrational spacings ( $\Delta E$ 's).

Progression I		Progression II	
$E$ (eV)	$\Delta E$ (eV)	$E$ (eV)	$\Delta E$ (eV)
8.720		8.837	
	0.234		0.201
8.954		9.038	
	0.235		0.210
9.189		9.248	
	0.231		0.201
9.420		9.449	
	0.225		0.196
9.645		9.645	
	0.231		0.196
9.876		9.841	
	$\langle \Delta E \rangle = 0.231^a$		$\langle \Delta E \rangle = 0.201^a$

<sup>a</sup> $\langle \Delta E \rangle$  represents the average vibrational spacing.

mental frequencies<sup>10</sup> for  $\nu_7$  and  $\nu_9$ – $\nu_{12}$  are found to agree with the corresponding theoretical frequencies to within 3%. The normalized FCFs (nFCFs) calculated in the energy range of 0.000–1.225 eV above the IE( $C_3H_3$ ) or from the VUV energy of 8.964–9.900 eV are plotted as the stick diagram in Fig. 2. Here, the nFCFs are obtained by arbitrarily normalizing the FCF for the origin band or 0-0 transition to unity. Part of these nFCFs with values greater than 0.013 in the energy range of 0.000–0.620 eV (0–5000  $cm^{-1}$ ) above the IE( $C_3H_3$ ) are also given in Table III. The calculation shows that the 0-0 transition has the overwhelming FCF. The observation of only a minute steplike feature at the ionization onset in Fig. 3 is consistent with the conclusion that direct photoionization only plays a minor role in the photoionization of  $C_3H_3$  near its ionization threshold. As shown in Fig. 2, the nFCF plot reveals clusters of energy regions at which  $C_3H_3^+$  can be formed in Franck-Condon-allowed vibrational states with high probabilities. Interestingly, the positions of the autoionization peaks resolved in the VUV-PIE spectrum of  $C_3H_3$  are found to match the cluster pattern of the calculated nFCFs, pointing to the conclusion that the observed autoionization features are favorably promoted by the resonance-enhanced autoionizing mechanism.<sup>26</sup> We note that the theoretical energies of higher vibrational levels at energies greater than 0.5 eV above the IE( $C_3H_3$ ) are expected to be less accurate, and thus, the cluster pattern of nFCFs at VUV energies  $>9.2$  eV could be slightly shifted from the predicted positions shown in Fig. 2.

Figures 4(a)–4(d) depict the VUV-PIE spectra for the mass 39 ions in the VUV energy range of 8.0–11.0 eV observed in flames I, II, III, and IV, respectively. All these VUV-PIE spectra are found to have the same photoionization threshold (or IE value) at 8.67 eV and exhibit pronounced autoionizing structures in the regions of 8.7–10.0 eV. This observation indicates that the mass 39 ions observed in flames I–IV are mostly formed by the VUV photoionization of the same chemical species. The pattern of autoionizing features resolved in the region of 8.6–10.0 eV in the spectra of Figs. 4(a)–4(d) is found to be similar to those resolved in the VUV-PIE spectrum of Fig. 3. This, together with the IE value observed in the VUV-PIE spectra of Figs. 4(a)–4(d), provides for an unambiguous identification of  $C_3H_3$  in flames I–IV. The comparison of the VUV-PIE data in the region of 8.6–10.0 eV shown in these figures also provides information on the relative intensities of  $C_3H_3$  produced in flames I–IV. Under the flow conditions specified in Table I, the observed VUV-photoion spectra of Figs. 4(a)–4(d) yield the relative intensities of  $C_3H_3$  in flames I–IV to be flame I: flame II: flame III: flame IV  $\approx 2.5:2.2:1.6:1.0$ . The higher concentration of  $C_3H_3$  observed in the benzene flame suggests that propargyl radicals can be produced by the pyrolysis of benzene. We note that the VUV-PIE spectra for the mass 39 ions observed in different flames by the flame-sampling group at the ALS also reveals pronounced autoionization structures similar to those shown in Figs. 4(a)–4(d), indicating that the mass 39 ions observed are mostly due to the photoionization of  $C_3H_3$ .<sup>27</sup>

The  $C_3H_3^+$  cation produced by the VUV photoionization of  $C_3H_3$  is not the most stable  $C_3H_3^+$  cation. The cycloprope-

TABLE III. Theoretical normalized Franck-Condon factors (nFCFs) in the energy range of 0–5000  $cm^{-1}$  (0–0.62 eV) above the IE of  $C_3H_3$ . The FCF for the 0-0 transition is arbitrarily normalized to unity. The vibrational frequencies for  $C_3H_3^+$  used are anharmonic vibrational frequencies calculated at the B3LYP/6-311G(2df,p) level of theory (see the text).

nFCF	Energy <sup>a</sup> ( $cm^{-1}$ )	Quanta of vibration modes <sup>b</sup>				
1.000	0	00000	00000	00		
0.147	556	20000	00000	00		
0.111	662	02000	00000	00		
0.134	949	01100	00000	00		
0.036	1139	00000	01000	00		
0.218	1177	10010	00000	00		
0.016	1218	22000	00000	00		
0.346	1345	01001	00000	00		
0.193	1391	10000	10000	00		
0.020	1505	21100	00000	00		
0.016	1798	00020	00000	00		
0.024	1839	12010	00000	00		
0.019	1898	02200	00000	00		
0.051	1901	21001	00000	00		
0.022	2053	12000	10000	00		
0.021	2089	00000	00010	00		
0.029	2126	11110	00000	00		
0.046	2226	00000	20000	00		
0.027	2278	00000	02000	00		
0.093	2294	02101	00000	00		
0.026	2340	11100	10000	00		
0.029	2354	20020	00000	00		
0.075	2522	11011	00000	00		
0.096	2568	20010	10000	00		
0.379	2579	00000	01100	00		
0.101	2690	02002	00000	00		
0.067	2736	11001	10000	00		
0.056	3135	20000	01100	00		
0.042	3241	02000	01100	00		
0.015	3246	22002	00000	00		
0.015	3390	01000	00000	10		
0.020	3471	12111	00000	00		
0.051	3528	01100	01100	00		
0.016	3571	01001	20000	00		
0.018	3685	12101	10000	00		
0.030	3718	00000	02100	00		
0.083	3756	10010	01100	00		
0.022	3867	12012	00000	00		
0.033	3913	21011	10000	00		
0.131	3924	01001	01100	00		
0.073	3970	10000	11100	00		
0.019	4081	12002	10000	00		
0.053	4115	00000	01001	00		
0.019	4178	00000	00020	00		
0.064	4365	00000	01000	01		
0.019	4480	21001	01100	00		
0.016	4735	02001	00000	10		
0.018	4805	00000	21100	00		
0.035	4873	02101	01100	00		

<sup>a</sup>Energy measured with respect to the IE of  $C_3H_3$ .

<sup>b</sup>Number of quanta for the vibrational modes of ( $\nu_1 \nu_2 \nu_3 \nu_4 \nu_5 \nu_6 \nu_7 \nu_8 \nu_9 \nu_{10} \nu_{11} \nu_{12}$ ) for  $C_3H_3^+$ .

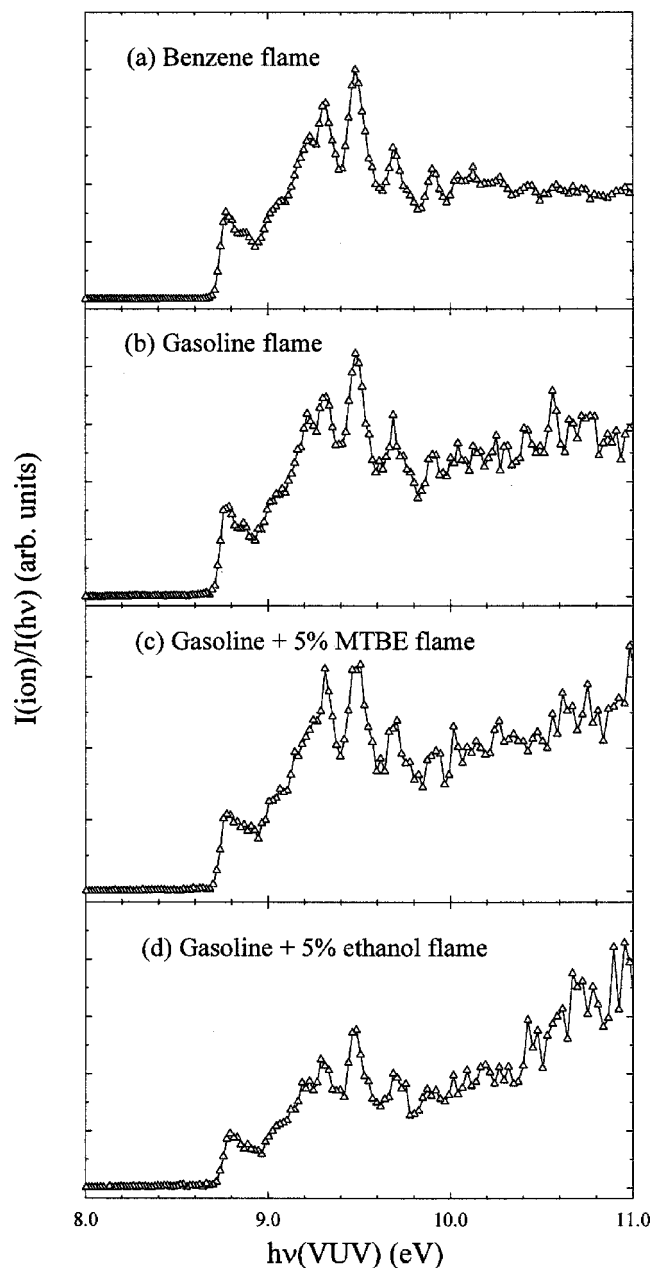


FIG. 4. VUV-photoion spectra for mass 39 cations recorded in the VUV synchrotron-based photoionization mass spectrometric sampling of (a) the benzene/oxygen flame, (b) the gasoline flame, (c) the gasoline+5% MTBE flame, and (d) the gasoline+5% ethanol flame. Note that the photoion intensities have been normalized by the corresponding VUV intensities detected by the silicon photodiode.

anium ion ( $c\text{-C}_3\text{H}_3^+$ ) is the global minimum on the  $\text{C}_3\text{H}_3^+$  potential surface<sup>28</sup> and is expected to be produced by the dissociative photoionization of larger hydrocarbon species formed in flames. On the basis of known heats of formation<sup>27</sup> for propargyl chloride,  $c\text{-C}_3\text{H}_3^+$ , and Cl atom, we estimate that the formation of  $c\text{-C}_3\text{H}_3^+$  by the dissociative photoionization of propargyl chloride can contribute to the mass 39 ions observed at VUV energies  $\geq 10.7$  eV.

By normalizing the PIE values for the first autoionization peaks of the VUV-PIE spectra of Fig. 3 and Figs. 4(a)–4(d), we find that these spectra are different at higher VUV energies. The comparison of the normalized PIE data provides clear evidence that the photoionization of other

chemical species also contributes to the intensities of mass 39 ions observed at higher VUV energies. Furthermore, the intensities of such background ions are in the following order: flame I < flame II < flame III < flame IV. The background ions contributing to the mass 39 ion signal in flames I–IV could include  $c\text{-C}_3\text{H}_3^+$ , which can be produced by the dissociative photoionization processes of larger hydrocarbon species formed in the premixed flames.

The discrepancies observed between the PIE spectra measured in the flames and photodissociation experiments can also arise from the differences in vibrational temperatures of propargyl samples. Propargyl radicals formed by chemical reactions in different flames are likely internally excited. If the vibrational excitations cannot be efficiently relaxed prior to the photoionization sampling, the vibrational temperatures for  $\text{C}_3\text{H}_3$  radicals observed in different flames might be different. Recent IR-VUV-PIE experiments show that the VUV-PIE measurement near the photoionization onset of a polyatomic species is not very sensitive to the vibrational energy content of the neutral species.<sup>15–17</sup> However, it is not unreasonable to expect that the PIE for vibrationally excited  $\text{C}_3\text{H}_3$  would increase at higher VUV energies compared to that for  $\text{C}_3\text{H}_3$  in the ground state.

#### IV. CONCLUSIONS

We have developed a pseudocontinuous effusive radical beam source based on known specificity of the excimer laser photodissociation processes. This source is applicable for the production of thermalized radicals with significant vibrational relaxation. The high duty factor achieved for the  $\text{C}_3\text{H}_3$  beam has made possible the efficient VUV-PIE measurement of  $\text{C}_3\text{H}_3$  using the high-resolution pseudocontinuous VUV synchrotron radiation source at the ALS. The VUV-PIE spectrum for  $\text{C}_3\text{H}_3$  thus obtained is found to be dominated by autoionizing Rydberg features, which are tentatively assigned as members of two vibrational progressions converging to excited vibronic states of  $\text{C}_3\text{H}_3^+$ . We have also presented the VUV-PIE spectra for mass 39 ions measured in the VUV synchrotron-based photoionization mass spectrometric sampling of combustion flames I–IV. The good agreements of the IE value and the pattern of autoionizing features observed in both the photodissociation and flames studies have provided for an unambiguous identification of  $\text{C}_3\text{H}_3$  in flames I–IV. The discrepancies observed between the VUV-PIE spectra at VUV energies above the  $\text{IE}(\text{C}_3\text{H}_3)$  obtained in flames and in photodissociation are attributed to higher vibrational excitations of  $\text{C}_3\text{H}_3$  formed in flames and/or dissociative photoionization processes involving larger hydrocarbon species produced in flames. This experiment also serves to show that combustion flames are a rich source of radicals for fundamental photoionization and photoelectron studies.

#### ACKNOWLEDGMENTS

This work was supported by the U.S. Department of Energy, Office of Basic Energy Sciences, Division of Chemical Sciences, Geosciences, and Biosciences under Contracts No. DE-FG02-02ER15306 (CYN), DE-AC02-05CH11231 (Lawrence Berkeley National Laboratory), and W-31-109-

ENG-38 (Argonne National Laboratory). One of the authors (C.Y.N.) also acknowledges partial support by the NSF Grant No. CHE-0517871, the AFOSR Grant No. F49620-03-1-0116 and the NSF Grant No. ATM-0317422. Another author (E.Q.) acknowledges support by CAS Grant No. 1731230600001, the NSFC Grant Nos. 20473081 and 20533040, and SRF for ROCS, SEM. Two of the authors (B.R. and M.L.M.) gratefully acknowledge the skillful help of Joseph Gregar, scientific glassblower at Argonne National Laboratory, in producing the original quartz tubes for the radical source with tight, mechanical-precision-like specifications. Portions of this research are related to the effort of a Task Group of the International Union of Pure and Applied Chemistry (2003-024-1-100), which focuses on the thermochemistry of chemical species implicated in combustion and atmospheric chemistry.

- <sup>1</sup>M. D. Smooke, R. J. Hall, M. B. Colket, J. Fielding, M. B. Long, C. S. McEnally, and L. D. Pfefferle, *Combust. Theory Modell.* **8**, 593 (2004).
- <sup>2</sup>C. A. Taatjes, N. Hansen, A. McIlroy *et al.*, *Science* **308**, 1887 (2005).
- <sup>3</sup>C. Y. Ng, *Adv. Photochem.* **22**, 1 (1997).
- <sup>4</sup>C.-W. Hsu, C.-L. Liao, Z.-X. Ma, and C. Y. Ng, *J. Phys. Chem.* **99**, 1760 (1995).
- <sup>5</sup>S. Nourbakhsh, K. Norwood, G.-Z. He, and C. Y. Ng, *J. Am. Chem. Soc.* **113**, 6311 (1991).
- <sup>6</sup>T. A. Cool, A. McIlroy, F. Qi, P. R. Westmoreland, L. Poisson, D. S. Peterka, and M. Ahmed, *Rev. Sci. Instrum.* **76**, 94102 (2005).
- <sup>7</sup>J. Berkowitz, *Photoabsorption, Photoionization, and Photoelectron Spectroscopy* (Academic, New York, 1979).
- <sup>8</sup>J. C. Robinson, N. E. Sveum, and D. M. Neumark, *J. Chem. Phys.* **119**, 5311 (2003).
- <sup>9</sup>D. A. Blank, W. Z. Sun, A. G. Suits, Y. T. Lee, S. W. North, and G. E.

- Hall, *J. Chem. Phys.* **108**, 5414 (1998).
- <sup>10</sup>T. Gilbert, R. Pfab, I. Fischer, and P. Chen, *J. Chem. Phys.* **112**, 2575 (2000).
- <sup>11</sup>K. C. Lau and C. Y. Ng, *J. Chem. Phys.* **122**, 224310 (2005).
- <sup>12</sup>G. R. Gladstone, M. Allan, and Y. L. Yung, *Icarus* **119**, 1 (1996).
- <sup>13</sup>J. M. Vrtilik, C. A. Gottlieb, E. W. Gottlieb, T. C. Killian, and P. Thaddeus, *Astrophys. J.* **346**, L53 (1990).
- <sup>14</sup>J. A. Miller and C. F. Melius, *Combust. Flame* **91**, 21 (1992).
- <sup>15</sup>X.-M. Qian, A. H. Kung, T. Zhang, K. C. Lau, and C. Y. Ng, *Phys. Rev. Lett.* **91**, 233001 (2003).
- <sup>16</sup>H. K. Woo, P. Wang, K.-C. Lau, X. Xing, C. Chang, and C. Y. Ng, *J. Chem. Phys.* **119**, 9333 (2003).
- <sup>17</sup>C. Y. Ng, *J. Electron Spectrosc. Relat. Phenom.* **142**, 179 (2005).
- <sup>18</sup>X. M. Qian, T. Zhang, C. Y. Ng, A. H. Kung, and M. Ahmed, *Rev. Sci. Instrum.* **74**, 2784 (2003).
- <sup>19</sup>X.-M. Qian, T. Zhang, C. Chang *et al.*, *Rev. Sci. Instrum.* **74**, 4096 (2003).
- <sup>20</sup>C. Y. Ng, *Adv. Ser. Phys. Chem.* **10A**, 394 (2000).
- <sup>21</sup>P. A. Heimann, M. Koike, C. W. Hsu *et al.*, *Rev. Sci. Instrum.* **68**, 1945 (1997).
- <sup>22</sup>B. Ruscic, H. Shang, C. Xu, and M. T. Berry (unpublished results); see also B. Ruscic, H. Shang, C. Xu, M. T. Berry, M. Litorja, and R. L. Asher, *Proceedings of the 56th International Symposium on Molecular Spectroscopy*, June 11–15, 2001, Columbus, OH, WH-13, p. 195.
- <sup>23</sup>T. Zhang, Ph.D. thesis, University of California, Davis, 2003.
- <sup>24</sup>J. A. R. Samson, *Techniques of Vacuum Ultraviolet Spectroscopy* (Wiley, New York, 1967).
- <sup>25</sup>The FCF calculation uses the MOMOCF program, which can be obtained from <http://hera.ims.ac.jp>
- <sup>26</sup>T. Baer and P. M. Guyon, in *High Resolution Laser Photoionization and Photoelectron Studies*, Wiley Series in Ion Chemistry and Physics, edited by I. Powis, T. Baer, and C. Y. Ng (Wiley, Chichester, 1995), p. 1.
- <sup>27</sup>T. A. Cool (private communication).
- <sup>28</sup>S. G. Lias, J. E. Bartmess, J. F. Liebman, J. L. Holmes, R. D. Levin, and W. G. Mallard, *J. Phys. Chem. Ref. Data Suppl.* **17**, 1 (1988).